

## Magnetic Ground State of an Experimental $S = 1/2$ Kagome Antiferromagnet

M. A. de Vries,<sup>1</sup> K. V. Kamenev,<sup>2</sup> W. A. Kockelmann,<sup>3</sup> J. Sanchez-Benitez,<sup>2</sup> and A. Harrison<sup>4,1,\*</sup>

<sup>1</sup>CSEC and School of Chemistry, The University of Edinburgh, Edinburgh, EH9 3JZ, United Kingdom

<sup>2</sup>CSEC and School of Engineering & Electronics, The University of Edinburgh, Edinburgh, EH9 3JZ, United Kingdom

<sup>3</sup>ISIS, STFC Rutherford Appleton Laboratory, Chilton, Didcot, OX11 0QK, United Kingdom

<sup>4</sup>Institut Laue-Langevin, 6 rue Jules Horowitz, F-38042 Grenoble, France

(Received 4 May 2007; revised manuscript received 20 September 2007; published 17 April 2008)

We present a detailed analysis of the heat capacity of a near-perfect  $S = 1/2$  kagome antiferromagnet, zinc paratacamite  $\text{Zn}_x\text{Cu}_{4-x}(\text{OH})_6\text{Cl}_2$ , as a function of stoichiometry  $x \rightarrow 1$  and for fields of up to 9 T. We obtain the heat capacity intrinsic to the kagome layers by accounting for the weak  $\text{Cu}^{2+}/\text{Zn}^{2+}$  exchange between the Cu and the Zn sites, which was measured independently for  $x = 1$  using neutron diffraction. The evolution of the heat capacity for  $x = 0.8 \dots 1$  is then related to the hysteresis in the magnetic susceptibility. We conclude that for  $x > 0.8$  zinc paratacamite is a spin liquid without a spin gap, in which unpaired spins give rise to a macroscopically degenerate ground state manifold with increasingly glassy dynamics as  $x$  is lowered.

DOI: 10.1103/PhysRevLett.100.157205

PACS numbers: 75.40.Cx, 75.30.Hx, 75.45.+j

Physical realizations of the  $S = 1/2$  kagome Heisenberg antiferromagnet have been long sought after because it is expected that the ground state of this system can retain the full symmetry of the underlying effective magnetic Hamiltonian [1,2]; the geometry of the kagome lattice frustrates the classical Néel antiferromagnetic ordering, and no symmetry-breaking transition is expected even at  $T = 0$  [3–7]. It has been suggested that even in the thermodynamic limit the symmetric quantum-mechanical electronic ground state is protected from quantum-mechanical dissipation [8] by a gap between the nonmagnetic ground state and the lowest magnetic (triplet) excitations [9,10]. In practice, however, a gap of order  $J/20$  [5] may be too small to expect a nonmagnetic ground state in real materials.

Shores *et al.* [11] have shown that in the Cu salt herbertsmithite [12]  $[\text{ZnCu}_3(\text{OH})_6\text{Cl}_2]$ , depicted in the inset of Fig. 1] antiferromagnetically coupled  $\text{Cu}^{2+}$  ions are located at the vertices of a kagome lattice. Muon experiments have shown that the ground state of this system is either paramagnetic or (quantum) spin liquid. Almost no muon relaxation was observed even at 50 mK [13], despite the large Weiss temperature  $\theta_w \approx -300$  K [11,14]. Separating the kagome layers are Zn sites of  $O_h$  symmetry, which can also host  $\text{Cu}^{2+}$  ions to form the zinc paratacamite family of stoichiometry  $\text{Zn}_x\text{Cu}_{4-x}(\text{OH})_6\text{Cl}_2$  with  $0.3 \leq x \leq 1$ . For  $\text{Zn}^{2+}$  stoichiometries  $x < 0.3$ , the Zn site is mainly occupied by Jahn-Teller active  $\text{Cu}^{2+}$  ions and becomes angle distorted. At this point the symmetry of the lattice changes from rhombohedral ( $x > 0.3$ ) to monoclinic, forming the end-member clinoatacamite [15]. Because of the strong Jahn-Teller distortion of the Cu sites on the kagome lattice, the mixing of  $\text{Cu}^{2+}$  and  $\text{Zn}^{2+}$  between the Cu and the Zn sites (antisite disorder) in the  $x = 1$  phase can be expected to be low, but exactly how low has not previously been measured. From the magnetic

susceptibility of samples with  $x < 1$  it is clear that the  $\text{Cu}^{2+}$  ions on the interplane Zn site are only weakly coupled to the kagome layers, and it has been suggested that the divergence of the magnetic susceptibility for  $x = 1$  at low temperatures can be explained by antisite permutations of 6%–7% of the  $\text{Cu}^{2+}$  ions with  $\sim 19\%$  of the  $\text{Zn}^{2+}$  [16–18].

To be able to account for the antisite disorder in the further analysis of the system, the  $\text{Cu}^{2+}/\text{Zn}^{2+}$  mixing was measured using neutron powder diffraction at the Rotax neutron time-of-flight diffractometer at the ISIS facility,

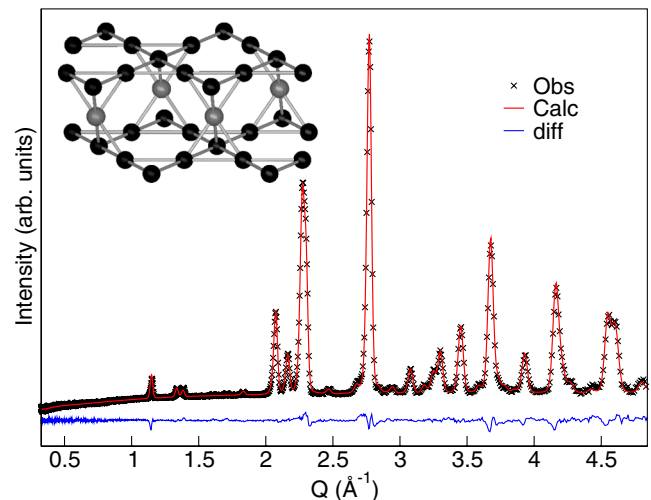


FIG. 1 (color online). Section of the neutron-diffraction pattern of  $\text{ZnCu}_3(\text{OD})_6\text{Cl}_2$  at 10 K, and the result of the structure refinement (residuals  $\chi^2 = 13.95$ ,  $R_p = 2.83\%$ ,  $R_{wp} = 2.73\%$ ). The inset shows two kagome layers with Cu sites (black), and the interplane Zn site (gray) of the zinc paratacamite structure. The antisite disorder means that a fraction of the  $\text{Cu}^{2+}$  ions interchange with (for  $x = 1$  an equal number of)  $\text{Zn}^{2+}$  ions.

United Kingdom. We used a 4 g powder sample of deuterated  $x = 1$  zinc paratacamite, synthesised using the hydrothermal method as described in [11]. The purity of the samples and  $\text{Cu}^{2+}$  to  $\text{Zn}^{2+}$  ratio were verified with powder x-ray diffraction and inductively coupled plasma auger electron spectroscopy (ICP-AES) with an accuracy of  $\pm 0.03$  in  $x$ . Neutron-diffraction data were collected at 285, 150, and 10 K, and Rietveld analyzed against the structure as reported in [11]. No structural changes were observed with temperature, and the level of deuteration was refined to 94.0(6)%. During the refinement the total  $\text{Cu}^{2+} : \text{Zn}^{2+}$  ratio was fixed at 3:1, as measured directly using ICP-AES. It was further assumed there were no vacant Zn or Cu sites. In this way the  $\text{Cu}^{2+}$  occupancy on the kagome lattice was refined to 91(2)%, corresponding to a  $\text{Zn}^{2+}$  occupancy of the interplane Zn site of 73(6)% [19], for the highest-statistics data set taken at 10 K. The result is given in Fig. 1. The refinements of the data taken at 150 and 285 K were in overall agreement within the experimental error. On relaxation of the constraints the solution was stable, but no longer unique. There was a small further reduction of the residues for a slight reduction of the Cu and Zn site occupancies, which also suggests that the experimental error will be larger than stated.

The heat-capacity measurements were carried out using a Quantum Design PPMS system, on  $\sim 5$  mg dye-pressed pellets of  $\text{Zn}_x\text{Cu}_{4-x}(\text{OH})_6\text{Cl}_2$  with  $x = 0.5, 0.8, 0.9$  and 1.0. We could reproduce the heat capacity for  $x = 1$  in 0, 1, 2, 3, 5, 7 and 9 T fields as reported by Helton *et al.* [14]. Figure 2 presents the heat capacities of samples with  $x = 0.8, 0.9$ , and  $x = 1$  in 0 and 9 T and for  $x = 0.5$  in 0 T. For intermediate fields, not shown here for clarity, the shoulder gradually moves to higher temperatures while the total entropy below  $\sim 24$  K remains constant. The magnetic susceptibility of samples with  $x = 0.8, 0.9$ , and  $x = 1$  as shown in Fig. 3 was measured with a Quantum Design MPMS system, on  $\sim 50$  mg pellets.

To the eye, the field dependence of the heat capacity is similar to the Schottky anomaly arising from defects in Zn-doped  $\text{Y}_2\text{BaNiO}_5$  and  $[\text{Ni}(\text{C}_2\text{H}_8\text{N}_2)_2(\text{NO}_2)]\text{ClO}_4$  (NENP) [20]. Hence, we have applied a similar analysis as described in [20]. To study the field-dependent part of the heat capacity, for each sample ( $x$ ) the difference was taken between the interpolated heat capacity curves measured in different fields. The inset in Fig. 2 shows the difference between the 0 and 9 T curves  $\Delta C_V/T = [C_V(H_1 = 0 \text{ T}) - C_V(H_2 = 9 \text{ T})]/T$  for  $x = 0.8$  (crosses) and for  $x = 1$  (squares). We found that the field-dependent part of the heat capacity can be modeled by a small number of zero-field split doublets, i.e., interacting  $S = 1/2$  spins or  $S = 1/2$  excitations.  $\Delta C_V/T$  was fitted with  $f[C_V^{S=1/2}(\Delta E_{H1}) - C_V^{S=1/2}(\Delta E_{H2})]/T$ , where  $f$  is the fraction of doublets per unit cell (or their spectral weight).  $C_V^{S=1/2}(\Delta E_H)$  is the heat capacity from a  $S = 1/2$  spin with

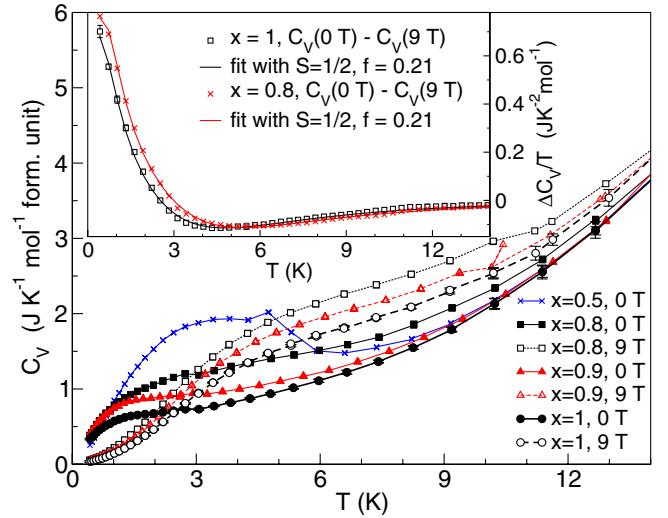


FIG. 2 (color online). The heat capacity in 0 T for samples with  $x = 0.5, 0.8, 0.9$ , and 1 as well as in 9 T for  $x = 0.8, 0.9$  and 1. The error bars are given for  $x = 1$  only. The inset displays  $\Delta C_V/T$  for  $x = 0.8$  and  $x = 1$  and their respective fits.

a level splitting  $\Delta E_H$ , which for fields  $H \geq 2$  T, equals the Zeeman splitting with  $g \approx 2.2$ , as shown in the inset of Fig. 4. The shoulder in the heat capacity in zero-field, which corresponds to a zero-field splitting of the doublets of  $\Delta E \sim 1.7$  K (0.15 meV) for  $x = 1$ ,  $\Delta E \sim 2.1$  K for  $x = 0.9$  and  $\Delta E \sim 2.2$  K for  $x = 0.8$  indicates that the levels involved are part of an interacting system, and cannot be ascribed to a paramagnetic impurity phase. The best agreement with experiment was obtained when a small Gaussian spread  $\sigma$  in level splittings  $\Delta E$  was taken into account, indicated as the error bars in the inset of Fig. 4. This brings the number of fit parameters to 5. The lines through the data points in the inset of Fig. 2 are the fit results for  $x = 0.8$  and  $x = 1$ . We find that  $f = 0.21(1), 0.22(1)$ , and

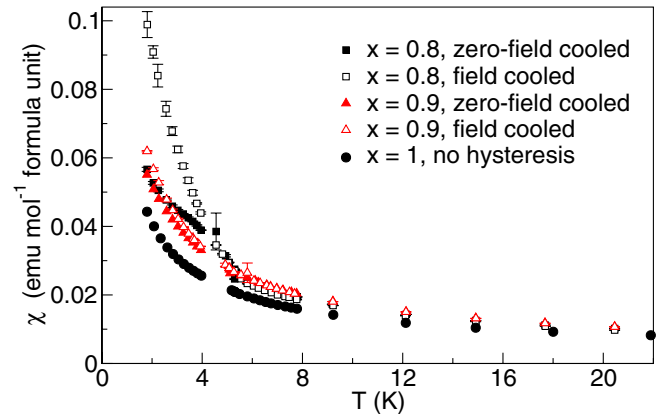


FIG. 3 (color online). The zero-field cooled and field cooled magnetic susceptibility for zinc paratacamite with  $x = 0.8$  and  $x = 0.9$ , compared with the susceptibility for  $x = 1$  which has a negligible hysteresis.

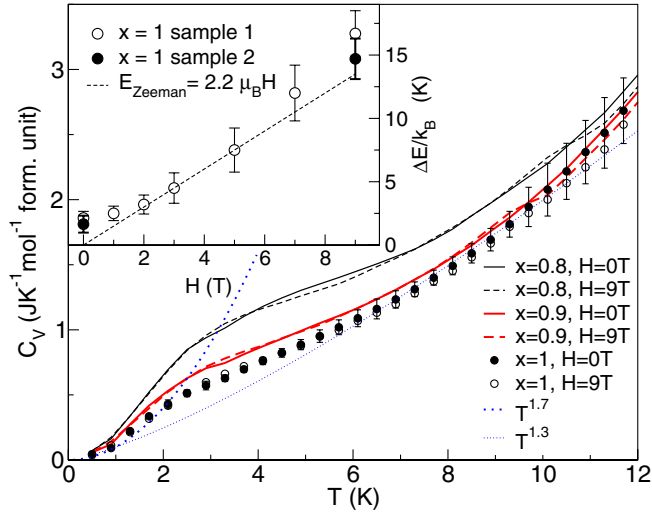


FIG. 4 (color online). The field-independent part of the heat capacity as obtained from the 0 and 9 T data of samples with  $x = 0.8, 0.9$ , and 1. The dotted lines (blue online) give fits to the corrected heat capacity for  $x = 1$  with  $\gamma T^\alpha$  with  $\alpha = 1.3$  and 1.7. The inset shows  $\Delta E$  as a function of  $H$  between 0 and 9 T, compared to the Zeeman splitting with  $g = 2.2$ . Sample 2 is the deuterated  $x = 1$  sample which was used in the neutron-diffraction experiment.

0.19(1) for  $x = 0.8, 0.9$ , and 1.0, respectively. For  $x = 1$ , with three  $\text{Cu}^{2+}$  ions per unit cell, this accounts on average for 6.0(6)% of all  $\text{Cu}^{2+}$ .

Because of a spin gap the heat capacity of the  $S = 1/2$  kagome antiferromagnet is expected to show a shoulder between  $J/20$  and  $\sim J/10$  corresponding to the population of the lowest magnetic ( $S_{\text{tot}} = 1$ ) levels [5–7,21]. In our data a shoulder is evident in zero field. However, with the application of a magnetic field this shoulder moves to higher temperatures (energies), as shown in the inset of Fig. 4. This is very different from what can be expected for, for example, a singlet-triplet system with a nonmagnetic ground state. For the latter an applied field will lower the energy of the  $S = 1$  level with spin aligned along the field, so that for sufficiently strong fields a level crossing occurs and this  $S = 1$  level will become the ground state. It is clear that such a level crossing is not observed here. Most likely, the lowest energy level involved in the system giving rise to a field dependence is a magnetic level too. Several models have been tried, of which only the doublet (a  $S = 1/2$  system) gives an overall consistent fit for all 18 curves from a total of 5 samples, for each model using only 5 fitting parameters. A model with a triplet of  $S = 1$  levels results in a slightly poorer fit to the data as compared with a doublet. Similar models with higher-level multiplets ( $S_{\text{tot}} > 1$ ) can not be brought into agreement with our data. It should be noted that a doublet with a field dependence as described here has also been observed in neutron spectroscopy data [14,22]. As is shown in Fig. 3, the system gradually develops a magnetic hysteresis as  $x$  is

lowered (the  $\text{Cu}^{2+}$  concentration is increased), while the muon relaxation increase is indicative of a slowing down of the spin dynamics [13]. The hysteresis is a history dependence which rules out a macroscopic quantum state for the system as a whole, since such a state would have a unitary time evolution as described by the Schrödinger equation. That the latter is not the case here is also clear from the energy gap for the antisite spins in zero field, which increases as  $x$  is lowered. Using our model this increase is quantified as a gap of 1.7 K for  $x = 1$  to 2.2 K for  $x = 0.8$ . This may be the strongest indication that the energy gap corresponds to local excitations rather than coherent many-body quantum states of the total system. In the latter case, the time dependence should follow the Schrödinger equation where a larger gap leads to faster dynamics.

We suggest, as is also done in [16–18], that the fraction  $f$  of zero-field split doublets, which models the field dependence in the heat capacity for  $0.8 \leq x \leq 1$ , are weakly coupled  $S = 1/2$  spins from  $\text{Cu}^{2+}$  ions residing on inter-plane Zn sites (antisite spins). For  $x = 1$  an identical fraction  $f$  of  $\text{Zn}^{2+}$  ions must occupy Cu sites on the kagome lattice. Once  $f(x)$  is known the  $\text{Cu}^{2+}$  coverage  $c(x)$  of the three Cu sites per unit cell is given by  $c = 4 - x - f(x)$ . An important assumption in our argument is that the heat capacity of a slightly diamagnetically doped kagome lattice is field independent, which is reasonable as long as  $g\mu_B H \ll \theta_w$  [6,23]. For the deuterated  $x = 1$  sample used for the neutron-diffraction measurements it follows that the antisite disorder is 6.3(3)% in  $\text{Cu}^{2+}$  or 19.0(9)% in  $\text{Zn}^{2+}$ , in rough agreement with the neutron-diffraction result.

Comparing the heat capacity data of several  $x = 1$  samples, all synthesized at a temperature of 484 K, an average antisite disorder of  $\sim 6.0(6)\%$  in  $\text{Cu}^{2+}$  is derived, as listed in Table I, along with the results for  $x = 0.8$  and  $x = 0.9$ . The chemical potential behind the  $\text{Cu}^{2+}/\text{Zn}^{2+}$  partitioning can now be estimated to  $\sim 1400$  K, a plausible value given that most likely the Zn site becomes locally slightly angle-distorted, if occupied by an otherwise orbitally degenerate  $\text{Cu}^{2+}$  ion. The Cu sites on the kagome lattice are energetically favored by the  $\text{Cu}^{2+}$  ions, and there is only a slow increase of the  $\text{Cu}^{2+}$  occupancy on the Zn sites until the  $\text{Cu}^{2+}$  occupancy of the kagome lattice ( $c$  in Table I) is almost complete. For  $x = 0.8$  the magnetic hysteresis is too large to be ascribed to impurities or local variations in Zn stoichiometry (Fig. 3). Since even at  $x = 0.8$  only  $\sim 20\%$  of the Zn sites are occupied by  $\text{Cu}^{2+}$ , this hysteresis must be due to the higher connectivity of the 3D lattice, which is mainly due to the higher  $\text{Cu}^{2+}$  occupancy of the kagome planes (see Table I). Hence, for the phases  $x < 1$  which have a magnetic hysteresis the kagome layers must be in a magnetic state; i.e., both singlet and triplet states mix into the ground state. Since no quantum phase transition occurs between  $x = 0.8$  and  $x = 1$  as is clear from our heat-capacity data, the ground state of the ka-

TABLE I. The fitted fraction of antisite spins per unit cell  $f$ , the corresponding  $\text{Cu}^{2+}$  occupancy of the kagome lattice  $c = 4 - x - f$ , the total entropy from the antisite spins  $\mathcal{S}_f$ , the measured total entropy  $\mathcal{S}(T)$  up to 24 K, and the percentage of the entropy recovered per  $\text{Cu}^{2+}$  spin.

$x$	$f$	$c$	$\mathcal{S}_f/R$	$\mathcal{S}(T)/R$	$\frac{\mathcal{S}(T)}{(4-x)\ln(2)}$
$\pm 0.03$	$\pm 0.018$	$\pm 0.03$	$f \ln(2)$	@ $T = 24$ K <sup>b</sup>	%
0.50	0.50 <sup>a</sup>	3.00	0.346(8)	1.061(12)	43.9(2)
0.80	0.210	2.97	0.15	0.993(11)	44.7(2)
0.90	0.220	2.88	0.15	0.959(9)	44.8(2)
1.00	0.190	2.81	0.13	0.933(9)	44.8(2)

<sup>a</sup>Here  $f$  was not obtained from the heat capacity, which at this level of doping is altered due to a cooperative transition. However, for  $x = 0.5$  it is safe to assume that  $c = 3.0$  (full occupancy) and hence  $f = x$ .

<sup>b</sup>For  $T > 24$  K no relative changes in  $\mathcal{S}(T)$  occur between samples with different  $x$ .

some layers in the  $x = 1$  phase must be magnetic too. This is in support of NMR measurements [24,25] in that there is no spin gap. What is remarkable in the present case is that the appearance of unpaired spins precedes the breaking of spin-rotational symmetry to a long-range ordered state. This results in a macroscopically degenerate ground state with increasingly glassy dynamics as  $x$  is lowered.

The heat capacity of the kagome lattice can be estimated by subtracting the heat capacity from the  $\text{Cu}^{2+}$  spins on the Zn sites. The result for the data with  $0.8 \leq x \leq 1$  is shown in Fig. 4. For all  $x$  the curves obtained from the 0 and 9 T data are identical within the experimental error, which follows from the quality of the fit as described in the previous paragraphs. This part of the heat capacity most likely corresponds to the kagome layers. In this field-independent part of the heat capacity a weak shoulder is visible at a slightly higher temperature than the shoulder due to the antisite spins. As  $x \rightarrow 1$  the shoulder becomes less pronounced, and hence, it may be interpreted as due to the entropy release when the fluctuations in neighboring kagome layers, which are connected via the antisite spins, decouple. If the heat capacity from perfectly 2D kagome layers follows a power-law for  $T \rightarrow 0$ , then taking into account the distortive effect of the shoulder due to couplings between the kagome layers,  $0.1T^\alpha \text{ mol}^{-1}$  formula units with  $\alpha = 1.3(1)$  is our best estimate. An exponent  $\alpha = 2$  cannot be brought into agreement with our data.

In summary, based on the field dependence of the shoulder in the low-temperature heat capacity, which corresponds to the weakly dispersive feature observed at the Zeeman energy in neutron spectroscopy data, we rule out interpretations based on a singlet-triplet splitting. Rather, the feature remains a doublet over the entire range of

applied fields. We suggest these doublets are the magnetic states of the  $\text{Cu}^{2+}$  antisite spins, which raises an important question as to the origin of the observed zero-field splitting of the antisite spins. From analysis of the heat capacity and the magnetic susceptibility as a function of  $x$  we further conclude that even for  $x = 1$  the ground state of the kagome system is a gapless spin liquid.

We gratefully acknowledge helpful discussions with Philippe Mendels (Université Paris Sud), Paul Attfield, and Philippe Monthoux (the University of Edinburgh), Claudine Lacroix (Lab. Louis Néel), Frederick Mila, Andreas Läuchli and Henrik Rønnow (EPFL). We further acknowledge an EPSRC Grant No. EP/E06471X/1. M. dV. also thanks the ESF HFM network for an exchange grant.

\*a.harrison@ed.ac.uk

- [1] P. W. Anderson, *Science* **235**, 1196 (1987).
- [2] C. Lhuillier, *Lect. Notes Phys.* **595**, 161 (2002).
- [3] P. W. Leung and V. Elser, *Phys. Rev. B* **47**, 5459 (1993).
- [4] F. Mila, *Phys. Rev. Lett.* **81**, 2356 (1998).
- [5] C. Waldtmann *et al.*, *Eur. Phys. J. B* **2**, 501 (1998).
- [6] P. Sindzingre *et al.*, *Phys. Rev. Lett.* **84**, 2953 (2000).
- [7] B. H. Bernhard, B. Canals, and C. Lacroix, *Phys. Rev. B* **66**, 104424 (2002).
- [8] A. J. Leggett *et al.*, *Rev. Mod. Phys.* **59**, 1 (1987).
- [9] G. Misguich, V. Pasquier, F. Mila, and C. Lhuillier, *Phys. Rev. B* **71**, 184424 (2005).
- [10] L. B. Ioffe *et al.*, *Nature (London)* **415**, 503 (2002).
- [11] M. P. Shores, E. A. Nytko, B. M. Bartlett, and D. G. Nocera, *J. Am. Chem. Soc.* **127**, 13462 (2005).
- [12] R. Braithwaite, K. Mereiter, W. Paar, and A. Clark, *Mineral. Mag.* **68**, 527 (2004).
- [13] P. Mendels *et al.*, *Phys. Rev. Lett.* **98**, 077204 (2007).
- [14] J. S. Helton *et al.*, *Phys. Rev. Lett.* **98**, 107204 (2007).
- [15] X. G. Zheng *et al.*, *Phys. Rev. Lett.* **95**, 057201 (2005).
- [16] Y. Ran, M. Hermele, P. A. Lee, and X.-G. Wen, *Phys. Rev. Lett.* **98**, 117205 (2007).
- [17] G. Misguich and P. Sindzingre, *Eur. Phys. J. B* **59**, 305 (2007).
- [18] F. Bert *et al.*, *Phys. Rev. B* **76**, 132411 (2007).
- [19] The stated error bar is  $3 \times$  the  $\sigma$  estimated in the Rietveld refinement, corresponding to a 99% confidence interval.
- [20] A. P. Ramirez, S.-W. Cheong, and M. L. Kaplan, *Phys. Rev. Lett.* **72**, 3108 (1994).
- [21] G. Misguich and B. Bernu, *Phys. Rev. B* **71**, 014417 (2005).
- [22] S.-H. Lee *et al.*, *Nat. Mater.* **6**, 853 (2007).
- [23] A. P. Ramirez, B. Hessen, and M. Winklemann, *Phys. Rev. Lett.* **84**, 2957 (2000).
- [24] T. Imai, E. A. Nytko, B. M. Bartlett, M. P. Shores, and D. G. Nocera, *Phys. Rev. Lett.* **100**, 077203 (2008).
- [25] A. Olariu *et al.*, *Phys. Rev. Lett.* **100**, 087202 (2008).